

# Symbolical Analysis of RF-Network Problems using Mason's Rule

*Nikolai SCHWERG*

Radio-Frequency Group, European Organization for Nuclear Research (CERN), CH-1211 Geneve 23, Switzerland

nikolai.schwerg@cern.ch

**Abstract.** *We briefly review Mason's rule for the computation of RF-network problems and show its implementation into the software package freeMASON. This tool solves symbolically Mason's rule for any wave quantity and allows to derive analytical expressions as well as their functional evaluation. We demonstrate our approach studying the effect of an unbalanced magictee on the RF power distribution to two accelerating cavities.*

## Keywords

Mason's rule, symbolical network analysis, RF power distribution, S-parameters, flow graph.

## 1. Introduction

Particle accelerators use RF-systems for the acceleration of charged particles. The RF-system typically consists of an RF amplifier, transmission lines, a power distribution system, accelerating cavities, and a control and feed-back system. The number of cavities depends on the accelerator size and the required beam energy. In general we can distinguish two different system topologies: one transmitter/amplifier feeding a single cavity or one amplifier feeding several cavities [1]. In the latter case the RF power is split and distributed, *e.g.*, by means of waveguide systems such as magictees. The phase and amplitude of the accelerating field in the cavities is controlled by an RF feed-back system. Differences in the waveguide length to the cavities and especially unbalances in the power splitting have to be tightly controlled. In addition, the cavities are never identical and cause further variations in the field distribution. Phase differences can be adjusted using variable phase-shifters, compare *e.g.* [2]. Differences in amplitude are more difficult to mitigate.

The design and optimization of power distribution systems by means of standard numerical tools such as FDTD or FEM codes suffer from high computational effort, *e.g.* for the description of many meters of conventional waveguide, and the accurate resolution of the transmission phase in electrical long structures, *e.g.*, [3]. Numerical models of the different components may not always be available.

An RF network problem can be conveniently described and analyzed by means of scatter parameters [4] and flow graphs [5]. The former allow for a description of the different devices only by means of measured or model S-parameters, the latter can be calculated using, *e.g.*, Mason's rule [6], [7]. Interconnecting waveguides and cables are simplified as transmission lines. This way, the network problem can be solved analytically, however laborious it may be.

In this paper we show how the network analysis can be performed symbolically by a computer – without risk of any arithmetic errors – yielding analytical expressions for any of the transfer functions. Notice that a symbolic approach performs mathematical operations on the symbols of the different quantities without assigning any values. This has the following advantages in comparison to numerical computations:

- The effect of *all* parameters becomes evident as it can be tracked in the formulae.
- The complexity of the problem can be reduced by taking out parameters while maintaining full control over the model and its error.
- The analytical expressions for the transfer functions can be solved for certain parameter in order to chose the appropriate range or even prove mathematically that some states can not be obtained (if no solution exists).

The aforementioned method is well suited for the optimization of complex RF networks such as the Linac4 RF power distribution system [8], the identification of critical network components, or drawing up parameters for components within a multiple interconnected system.

## 2. RF Power Distribution System

Fig. 1 shows a simplified version of a power distribution problem. Two cavities are fed by an unbalanced, but otherwise ideal magictee (see Appendix). The magictee is fed by a klystron from the  $\Sigma$ -port (sum) and the  $\Delta$ -port (differential) is closed by a load of  $-30$  dB reflection at an arbitrary phase of zero degrees. The reflected phases of the two cavities,  $\phi_1$  and  $\phi_2$ , are depending on the power coupler, tuner position and the tune state of the cavity, and considered

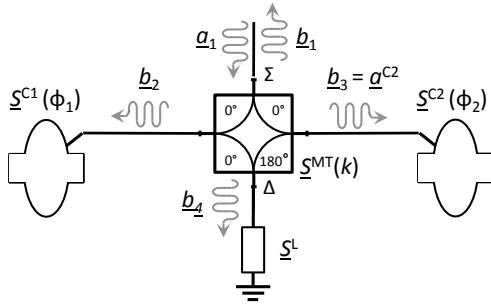


**Fig. 1.** RF-Network problem: Two cavities are fed by an ideal, but unbalanced magictee. The magictee is fed from the sum port while the differential port is closed by a load.

as variable for this example. Effects such as beam loading are disregarded and the magnitude of the reflection coefficient is assumed to be 1. The power splitting in the magictee can be varied from all power at port 3, *i.e.*,  $k = -1$ , to all power at port 2 for  $k = \sqrt{2} - 1$ . For  $k = 0$  the magictee is perfectly balanced.

In the following we investigate how the amplitude and phase of the waves fed to the two cavities,  $\underline{b}_2$  and  $\underline{b}_3$ , change with the unbalance  $k$  and the cavity reflection angles  $\phi_1$  and  $\phi_2$ . Furthermore we study the effect on the power reflected to the klystron,  $\underline{b}_1$ , and the power deposited in the load  $\underline{b}_4$ .

The chosen example is rather simple in order to facilitate the understanding of the presented method as well as to allow for comparison with other ways of computation. Nevertheless, the problem was triggered by work for the Linac4 high power RF distribution system [8].

### 3. Mason’s Rule

Mason’s rule is a technique to derive the transfer function of a given network or circuit problem from the flow graph. The rule is also known as non-touching loop rule or Mason’s gain formula [6], [7].

The **transfer function**  $T_{\underline{a}}^{\underline{b}}$  is the mathematical representation of the relation between an input quantity  $\underline{a}$  and output quantity  $\underline{b}$  of a linear time-invariant system in frequency domain, *e.g.*, the reflection and transmission coefficients of S-matrices.

A flow graph consists of **nodes** representing the network quantities such as forward and backward traveling waves, and **branches**, *i.e.* the directed, immediate and weighted connection between two nodes. In our example,  $\underline{a}_1$  and  $\underline{b}_1$  are nodes and every S-parameter constitutes a branch. Furthermore, the interconnection between two S-matrices by means of identities, *e.g.*  $\underline{b}_3 = \underline{a}^{C2}$ , defines a branch with weight 1. The flow graph of the network problem described above is shown in Fig. 2.

For the explanation of Mason’s rule we introduce the following terms: A **path**  $\mathcal{P}$  is an indexed list of unique

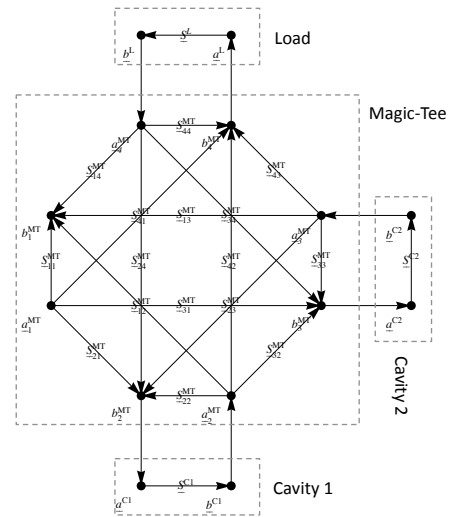


**Fig. 2.** Signal flow graph of the network problem in Fig. 1.

branches connecting two nodes. A path with identical start and end node is called a **loop**  $\mathcal{L}$ . Two paths/loops are denoted as **non-touching** if they do not have any *node or branch* in common. A set of  $n$  pair-wise non-touching loops is called a **multi-loop** of  $n$ -th order,  $\mathcal{L}^n$ . Loops are considered as multi-loops of 1<sup>st</sup> order.

The product of the weights of all branches of the path  $\mathcal{P}_i$  is called the **path product**  $\underline{P}_i$ . The product of the weights of the  $n$ -th order multi-loop,  $\mathcal{L}_j^n$ , is denoted as **loop product**  $\underline{L}_j^n$ . We further define  $\underline{L}^0 = 1$ . The transfer function  $T$  between the nodes  $\underline{a}$  and  $\underline{b}$  reads,

$$T_{\underline{a}}^{\underline{b}} = \frac{\sum_{i=1}^{\#\mathcal{P}} \underline{P}_i \sum_{n=0}^N (-1)^n \sum_{j=1}^{\#\mathcal{L}^n} \underline{L}_j^n |\mathcal{P}_i}{\sum_{n=0}^N (-1)^n \sum_{j=1}^{\#\mathcal{L}^n} \underline{L}_j^n} \quad (1)$$

where  $\#\mathcal{P}$  denotes the number of different paths  $\mathcal{P}_i$  between the two nodes,  $N$  the maximum order of multi-loops of the network and  $\#\mathcal{L}^n$  the number of multi-loops of order  $n$ . For a non-touching multi-loop  $\mathcal{L}_j^n$ . The expression  $\underline{L}_j^n |\mathcal{P}_i$  returns the loop product  $\underline{L}_j^n$  if  $\mathcal{P}_i$  and  $\mathcal{L}_j^n$  are non-touching and zero in all other cases.

### 4. freeMASON

Mason’s rule was implemented in the software package freeMASON [9] using the symbolic features of MATHEMATICA<sup>1</sup>. For a given flow graph freeMASON can construct the analytical expressions for the transfer function between any two nodes. The result can be used for functional analysis such as analytical minima determination, approximations and parametric plotting, or optimizations.

Based on user supplied sets of S-matrices and corresponding forward/backward traveling wave quantities a list of branches is created. The list is completed by identities

<sup>1</sup>WOLFRAM RESEARCH, INC., Mathematica Edition: Version 7.0, 2008.

```

FreeMason
MatrixSystems = {
  {
    {SMT1, SMT11, SMT12, SMT13, SMT14}, SMT1
    {SMT2, SMT21, SMT22, SMT23, SMT24}, SMT2
    {SMT3, SMT31, SMT32, SMT33, SMT34}, SMT3
    {SMT4, SMT41, SMT42, SMT43, SMT44}, SMT4
  },
  {{BSA1}, {{SSA11}}, {{ASA1}}, ...
};
Identities = {
  {BSA1, c, SMT2}, {SMT2, c, ASA1},
  ...
};
Coordinates = {
  {ASA1, {4, 1}},
  {BSA1, {5, 1}},
  ...
};
ReplacementVector = {ASA1 -> "a^C1", BSA1 -> "b^C1", ...}
BuiltNetwork[MatrixSystems, Identities, Coordinates, ReplacementVector];
DisplayNetwork[]
AnalyzeNetwork[]
TransferFunction = GetProduct[SMT1, SMT2];
    
```

**Fig. 3.** Example file using freeMASON from top to bottom: 1.) Defining a list of symbols for the S-Matrices and wave quantities, 2.) connecting the ports of the different  $n$ -ports by means of the in- and outgoing wave quantities, 3.) providing relative coordinates for all wave quantities allowing for graphical display of the flow chart, 4.) defining labels for the graphical display, 5.) automatic analysis of the network creating all paths and multi-loops, and 6.) determining of the transfer function between two wave quantities.

providing the interconnections of the different S-matrices, see Fig. 3. The input data can be verified by means of automatically created labeled flow graphs as shown in Fig. 2.

Starting once from every node, the graph is recursively traversed building a list of all possible paths. The recursion stops when no branch can be added to the current path without including a branch twice. It is worth mentioning that all comparisons are performed symbolically and therefore it can only be decided whether two symbols are identical, but not whether they are different. From the list of paths a list of loops can be extracted searching for all paths with identical start and end nodes. Every loop of  $m$  branches will be found exactly  $m$  times due to the way the list of paths is generated. Therefore, the list of loops is reduced to a list of unique loops.

The table of multi-loops is built from the list of unique loops in an iterative way: The list of unique loops is identical with the multi-loops of order 1. By pair-wise comparing multi-loop elements of order  $(n - 1)$  with elements of order 1, the non-touching multi-loops of  $n$ -th order are generated.

The transfer function between any two nodes is constructed by selecting the corresponding paths and multi-loops and building the symbolical expression according to (1). The result can be further reduced by replacing branches by their numerical values or using the powerful MATHEMATICA feature FullSimplify[. For a full numerical evaluation of the obtained expressions, e.g for plotting, the user has to provide values for the S-parameters from measurements, specification documents or numerical simulations.

Alternatively to the approach with Mason's rule, problems of concatenated S-matrices can be solved by means of the MATHEMATICA application CSC [10]. This approach is based on the analytical derivation of the S-matrix for the complete system taking into account the singularities of internal resonances. While CSC provides the full system matrix of the network problem, freeMASON returns only the transfer functions for beforehand selected nodes - at the interface, but also on the inside of the system.

### 5. Study of the Network Problem

We are now using Mason's rule and its implementation to solve the network problem. For a given input from the sum port  $a_1$  we determine the transfer functions to the two cavities,  $T_{a_1}^{b_2}$  and  $T_{a_1}^{b_3}$ , and to the load,  $T_{a_1}^{b_4}$ , as well as the reflection to the klystron,  $T_{a_1}^{b_1}$ . In the first case,  $T_{a_1}^{b_2}$ , we show all intermediate steps illustrating Mason's rule.

#### 5.1 Transfer Function between Klystron and Cavities

Fig. 4 shows the table of multi-loops detected for the network shown in Fig. 2. The number of unique loops or first order multi-loops is 8. The maximum order of multi-loops is 3, i.e. the combination of loop number 1, 6 and 8.

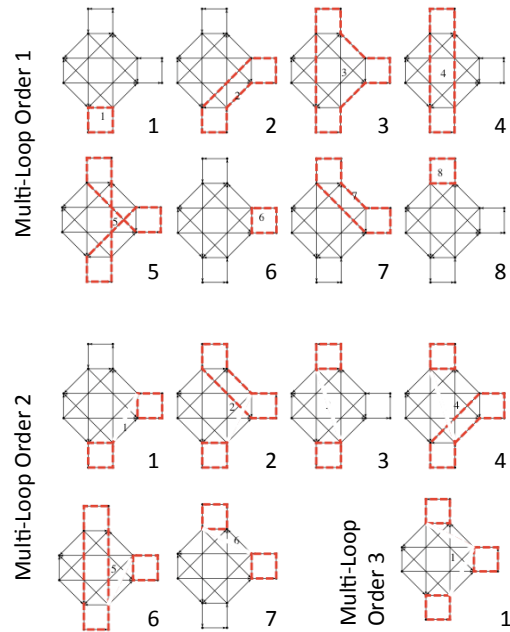


**Fig. 4.** Multi-Loops  $\mathcal{L}$  for the network in Fig. 2.

Between the nodes  $a_1$  and  $b^{C1}$  we can identify 5 different paths, see Fig. 5. Here path  $\mathcal{P}_1$  does not touch the 1<sup>st</sup> order multi-loops  $\mathcal{L}_6^1$ ,  $\mathcal{L}_7^1$  and  $\mathcal{L}_8^1$ , and the multi-loop of 2<sup>nd</sup> order  $\mathcal{L}_6^2$ . The path  $\mathcal{P}_2$  does not touch  $\mathcal{L}_8^1$  and path  $\mathcal{P}_4$  is non-touching to  $\mathcal{L}_6^1$  (see Figs. 4 and 5).

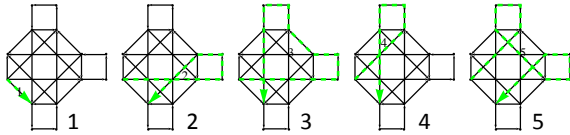


Fig. 5. All paths  $\mathcal{P}$  between the input from the klystron to cavity 1, i.e. between the nodes  $a_1$  and  $b_2$ .

The complete and symbolic expression for the transfer function  $T_{a_1}^{b_2}$  is bulky and shown only for educational interest in Fig. 6 (next page). Using, however, the values for the unbalanced magictee  $S^{MT}$  from (9), the transfer function can be greatly simplified,

$$T_{a_1}^{b_2} = \frac{S_{12}^{MT} (1 - S^L ((S_{12}^{MT})^2 + (S_{13}^{MT})^2) S^{C2})}{1 - S^L (S_{13}^{MT})^2 S^{C1} - S^L (S_{12}^{MT})^2 S^{C2}} \quad (2)$$

Fig. 7 shows the power transmitted to cavity 1 (modulus square of the transfer function) versus the unbalance  $k$  while varying the phase of the reflection of the cavity. In the same figure we show the power transmitted to cavity 2. For both, the phase of the reflection of cavity 2 is assumed to be constant  $0^\circ$ . Notice, that even in the case of an ideal and balanced magictee ( $k = 0$ ), the output to the two cavities shows different values depending on the phase difference of the reflected waves. This is due to the finite reflection of the load at the differential port.

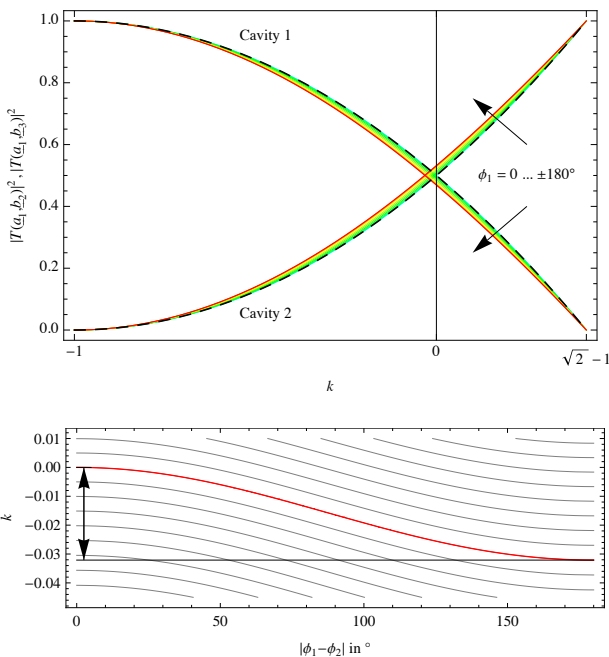


Fig. 7. (top) Power transfer to the two cavities versus unbalance  $k$  for different values of reflected phase from cavity 1,  $\phi_1 = -180^\circ \dots 180^\circ$ . The phase of the reflection from cavity 2 is assumed to be constant  $0^\circ$ . The dashed black lines indicate the transmission coefficients of the magictee,  $|S_{12}^{MT}|^2$  and  $|S_{13}^{MT}|^2$ , respectively. (bottom) Contour plot for the difference between the power fed to cavity 1 and 2. The gray lines represent an increase of the difference of 2% starting at 0 (red line). The arrow signifies the maximum range over which  $k$  can be used to compensate for power differences stemming from the phase-difference.

### 5.2 Compensating Amplitude Differences with the Magictee Unbalance

The unbalance of the magictee, if deliberately introduced, could be used to compensate for the aforementioned effect. Assuming a reflected phase  $\phi_2 = 0$  and using the parameters from (7) and (8), the ratio of the two transfer functions to the two cavities yields:

$$\begin{aligned} \frac{T_{a_1}^{b_2}}{T_{a_1}^{b_3}} &= \frac{S_{12}^{MT} (-1 + S^L ((S_{12}^{MT})^2 + (S_{13}^{MT})^2) S^{C2})}{S_{13}^{MT} (-1 + S^L ((S_{12}^{MT})^2 + (S_{13}^{MT})^2) S^{C1})} \\ &= \frac{\sqrt{1 - k(2+k)} \gamma}{1+k} \quad (3) \end{aligned}$$

where  $j$  is the imaginary unit and  $\gamma(\phi_1) = \frac{-1 + e^{j\phi_1} S^L}{-1 + S^L}$ . For an equal power distribution we solve the modulus of (3) to be 1:

$$k = \sqrt{2} \frac{|\gamma|}{\sqrt{1 + |\gamma|^2}} - 1 \quad (4)$$

For the presented example the power can be balanced between the two cavities for any value of  $\phi_1$  with values of  $k$  between 0 and  $-0.0321$ , see Fig. 7. Aiming for equal power and identical phase, (3)  $k$  becomes complex,

$$\underline{k} = \sqrt{2} \frac{\gamma}{\sqrt{1 + \gamma^2}} - 1 \quad (5)$$

and only returns real values for  $k(\phi_1 = 0) = 0$  and  $k(\phi_1 = 2.8241 \neq 0) = 0.1047$ . This means only for an ideal magictee and confirms the findings in the last paragraph. Notice, that only by means of the analytical approach we obtained the conditions for equal power splitting in magnitude and phase as well as the proof that the solution is unique.

### 5.3 Reflection and Load Deposition

Fig. 8 shows the reflection to the klystron as well as the transfer function from the klystron to the load. As could be expected from the high isolation of an ideal magictee fed from the sum port, the reflection decreases with increasing phase difference while the transfer to the differential port (load) increases. This characteristic weakens with increasing values of  $|k|$ . Notice that for  $k = 0$  and  $|\phi_1 - \phi_2| = 180^\circ$  the reflection to the klystron remains finite depending on the load properties.

## 6. Conclusion

Implementing the graphical Mason's rule into the symbolical environment of Mathematica allows to perform fully analytical evaluations of generic RF-network problems. Transfer functions are accessible for parametric studies, approximations and optimization. The influence of any property of the interconnected devices on the transfer function through the RF network can be analytically determined and

$$T_{a_1}^{b_2} = \frac{b_2}{a_1} = \frac{\begin{matrix} \mathbb{S}_{21}^{MT} \left[ \begin{matrix} +1 \\ -\mathbb{S}_{24}^{C_2 L \mathbb{S}_{23}^{MT} \mathbb{S}_{43}^{MT}} \\ -\mathbb{S}_{33}^{C_2 \mathbb{S}_{33}^{MT}} \\ -\mathbb{S}_{24}^{L \mathbb{S}_{24}^{MT}} \\ +\mathbb{S}_{24}^{C_2 L \mathbb{S}_{23}^{MT} \mathbb{S}_{44}^{MT}} \end{matrix} \right] + \mathbb{S}_{24}^{L \mathbb{S}_{24}^{MT} \mathbb{S}_{41}^{MT}} \left[ \begin{matrix} +1 \\ -\mathbb{S}_{33}^{C_2 \mathbb{S}_{33}^{MT}} \end{matrix} \right] + \mathbb{S}_{24}^{C_2 L \mathbb{S}_{23}^{MT} \mathbb{S}_{31}^{MT} \mathbb{S}_{43}^{MT}} + \mathbb{S}_{23}^{C_2 \mathbb{S}_{23}^{MT} \mathbb{S}_{31}^{MT}} \left[ \begin{matrix} +1 \\ -\mathbb{S}_{24}^{L \mathbb{S}_{24}^{MT}} \end{matrix} \right] + \mathbb{S}_{23}^{C_2 L \mathbb{S}_{23}^{MT} \mathbb{S}_{34}^{MT} \mathbb{S}_{41}^{MT}} \end{matrix}}{\begin{matrix} 1 - \left[ \begin{matrix} +\mathbb{S}_{23}^{C_1 \mathbb{S}_{23}^{C_2 L \mathbb{S}_{23}^{MT} \mathbb{S}_{34}^{MT} \mathbb{S}_{42}^{MT}} \\ +\mathbb{S}_{23}^{C_1 \mathbb{S}_{23}^{C_2 L \mathbb{S}_{23}^{MT} \mathbb{S}_{32}^{MT} \mathbb{S}_{43}^{MT}} \\ +\mathbb{S}_{23}^{C_1 \mathbb{S}_{23}^{C_2 L \mathbb{S}_{23}^{MT} \mathbb{S}_{32}^{MT} \mathbb{S}_{43}^{MT}} \\ +\mathbb{S}_{23}^{C_1 L \mathbb{S}_{23}^{MT} \mathbb{S}_{32}^{MT} \mathbb{S}_{44}^{MT}} \\ +\mathbb{S}_{24}^{C_1 \mathbb{S}_{24}^{MT} \mathbb{S}_{12}^{MT}} \\ +\mathbb{S}_{22}^{C_1 \mathbb{S}_{22}^{MT}} \\ +\mathbb{S}_{24}^{C_2 L \mathbb{S}_{23}^{MT} \mathbb{S}_{43}^{MT}} \\ +\mathbb{S}_{23}^{C_2 \mathbb{S}_{23}^{MT}} \\ +\mathbb{S}_{24}^{L \mathbb{S}_{24}^{MT}} \end{matrix} \right] + \left[ \begin{matrix} +\mathbb{S}_{23}^{C_1 \mathbb{S}_{23}^{C_2 L \mathbb{S}_{23}^{MT} \mathbb{S}_{33}^{MT} \mathbb{S}_{42}^{MT}} \\ +\mathbb{S}_{23}^{C_1 \mathbb{S}_{23}^{C_2 L \mathbb{S}_{23}^{MT} \mathbb{S}_{34}^{MT} \mathbb{S}_{43}^{MT}} \\ +\mathbb{S}_{23}^{C_1 \mathbb{S}_{23}^{C_2 L \mathbb{S}_{23}^{MT} \mathbb{S}_{32}^{MT} \mathbb{S}_{44}^{MT}} \\ +\mathbb{S}_{23}^{C_1 \mathbb{S}_{23}^{C_2 L \mathbb{S}_{23}^{MT} \mathbb{S}_{33}^{MT} \mathbb{S}_{44}^{MT}} \\ +\mathbb{S}_{23}^{C_1 \mathbb{S}_{23}^{C_2 L \mathbb{S}_{23}^{MT} \mathbb{S}_{33}^{MT} \mathbb{S}_{44}^{MT}} \\ +\mathbb{S}_{23}^{C_1 \mathbb{S}_{23}^{C_2 L \mathbb{S}_{23}^{MT} \mathbb{S}_{33}^{MT} \mathbb{S}_{44}^{MT}} \\ +\mathbb{S}_{23}^{C_2 L \mathbb{S}_{23}^{MT} \mathbb{S}_{33}^{MT} \mathbb{S}_{44}^{MT}} \end{matrix} \right] - \mathbb{S}_{23}^{C_1 \mathbb{S}_{23}^{C_2 L \mathbb{S}_{23}^{MT} \mathbb{S}_{33}^{MT} \mathbb{S}_{44}^{MT}} \end{matrix}}$$

**Fig. 6.** Symbolical expression for the transfer function  $T_{a_1}^{b_2}$  between the input from the klystron to cavity 1. Notice that the squared brackets [...] are used to structure the expression. The different terms in the sums are sorted by the respective order of the multi-loop. The first summand on the numerator consists of the path  $\mathcal{P}_1$  and all multi-loops ( $\mathcal{L}^0 = 1, \mathcal{L}_6^1, \mathcal{L}_7^1, \mathcal{L}_8^1, \mathcal{L}_7^1$ ) with sign according to their order.

evaluated. This can significantly reduce the computational effort compared to numerical parametric scans, especially for problems with many parameters. Furthermore, the analytical expression for the transfer function allows for the identification of internal resonant loops.

A magictee with a small, yet controlled unbalance can be used to compensate for power deviations due to phase differences. The power splitting between sum and differential port with phase difference of the signals from the two output ports changes with increasing unbalance in favor of the sum port.

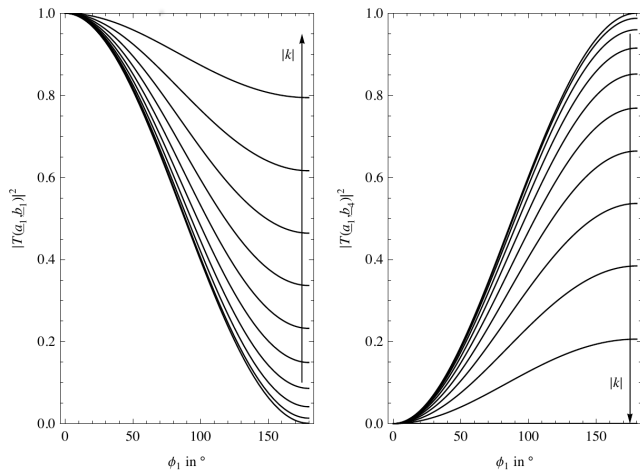


**Fig. 8.** (left) Reflected power to the klystron for different values of  $k = -1 \dots \sqrt{2} - 1$  and  $|\phi_1 - \phi_2|$ . (right) Power transmission to the load for the same input parameters.

## References

- [1] VALUCH, D. *High CW Power, Phase and Amplitude Modulator Realized with Fast Ferrite Phase-Shifters*. PhD thesis. Bratislava (Slovakia): Slovak University of Technology, 2004.
- [2] FRISCHHOLZ H. Generation and distribution of radio-frequency power in LEP. *IEEE Transactions on Nuclear Science*, 1985, vol. 32, no. 5, p. 2791 - 2793.

- [3] HADI, M. F., PIKET-MAY, M. A modified FDTD (2, 4) scheme for modeling electrically large structures with high-phase accuracy. *IEEE Transactions on Antennas and Propagation*, 1997, vol. 45, no. 2, p. 254 - 263.
- [4] KUROKAWA, K. Power waves and the scattering matrix. *IEEE Transactions on Microwave Theory and Techniques*, 1965, vol. 13, no. 2, p. 194 - 202.
- [5] Hewlett Packard. *S-parameter design, Application Note 154*. 1990.
- [6] MASON, S. J. Feedback theory - some properties of signal flow graphs. *Proceedings of the IRE*, 1953, vol. 41, no. 9, p. 1144 - 1156.
- [7] MASON, S. J. Feedback theory - further properties of signal flow graphs. *Proceedings of the IRE*, 1956, vol. 44, no. 7, p. 920 - 926.
- [8] BRUNNER, O., SCHWERG, N., CIAPALA, E. RF power generation in Linac4. In *Proceedings of 25th Linear Accelerator Conference*. Tsukuba (Japan), 2010.
- [9] SCHWERG, N. *freeMASON 1.0: Software Package for Mathematica 7.0*. 2012. (contact author for free download).
- [10] GLOCK, H.-W., ROTHMUND, K., VAN RIENEN, U. CSC - a procedure for coupled S-Parameter calculations. *IEEE Transactions on Magnetics*, 2002, vol. 38, no. 2, p. 1173 - 1176.

## Appendix

We define an magictee as ideal, if it is symmetric, loss-free and reciprocal. The ports 1 and 4 are also denoted as sum and differential port, respectively. The S-matrix is given by

$$S_{\text{ideal}} = \frac{1}{\sqrt{2}} \begin{pmatrix} 0 & 1 & 1 & 0 \\ 1 & 0 & 0 & 1 \\ 1 & 0 & 0 & -1 \\ 0 & 1 & -1 & 0 \end{pmatrix}. \quad (6)$$

The S-matrix for the ideal magictee, (6), can be modified in order to include an unbalance between the ports 2 and 3. We arbitrarily add a term  $\frac{k}{\sqrt{2}}$  to  $S_{12}^{\text{ideal}}$ ,

$$S_{12}^{\text{MT}} = S_{12}^{\text{ideal}} + \frac{k}{\sqrt{2}} = \frac{1+k}{\sqrt{2}} \quad (7)$$

with  $k$  between 0 for balanced output and  $\sqrt{2} - 1$  for output only to port 2. For a loss-free network the S-matrix fulfills the condition  $S^{\text{MT}}((S^{\text{MT}})^T)^* = 1$ . This results in

$$S_{13}^{\text{MT}} = \pm \sqrt{1 - (S_{12}^{\text{MT}})^2} = -\sqrt{\frac{1 - 2k - k^2}{2}}, \quad (8)$$

deciding for the negative sign in the second term. Both coefficients are displayed in Fig. 7. Alternately applying the loss-free and reciprocity condition,  $S_{ij}^{\text{MT}} = S_{ji}^{\text{MT}}$ , we obtain:

$$S^{\text{MT}} = \begin{pmatrix} 0 & S_{12}^{\text{MT}} & S_{13}^{\text{MT}} & 0 \\ S_{12}^{\text{MT}} & 0 & 0 & S_{13}^{\text{MT}} \\ S_{13}^{\text{MT}} & 0 & 0 & -S_{12}^{\text{MT}} \\ 0 & S_{13}^{\text{MT}} & -S_{12}^{\text{MT}} & 0 \end{pmatrix}. \quad (9)$$

## About Authors...

**Nikolai SCHWERG** received his Diploma and PhD electrical in engineering from the Technical University of Berlin (Germany) in 2006 and 2009, respectively. His research interests include numerical and analytical calculations of high power RF systems for accelerators and superconducting accelerator magnets.